Cocrystallization with Acetylene. The 1:1 Complex with Benzene: Crystal Growth, X-Ray Diffraction and Molecular Simulations[1])

by **Roland Boese***[a]), **Timothy Clark***[b]), and **Angelo Gavezzotti***[c])

[a]) Institut für Anorganische Chemie, Universität Essen, Universitätsstr. 3–5, D-45117 Essen
[b]) Computer-Chemie-Centrum, Universität Erlangen-Nürnberg, Nägelsbachstr. 25, D-91052 Erlangen
[c]) Dipartimento di Chimica Strutturale e Stereochimica Inorganica, Università di Milano, I-20133 Milano

Dedicated to Professor *Jack D. Dunitz* on the occasion of his 80th birthday

The crystal structure of an unusual 1:1 molecular complex between benzene and acetylene, two very small and apolar molecules, has been determined by X-ray-analysis of crystals grown by first mixing the two liquids under conditions of low temperature and high pressure in a capillary, followed by repeated zone melting to form crystals directly on the goniometer head of a diffractometer. Each acetylene molecule is clamped between two parallel benzene rings, with its molecular axis apparently perpendicular to the benzene planes. Closer inspection of thermal-motion data from the diffraction experiment suggests that the acetylene molecule undergoes a wobbling, or precession, motion between the two rings so that it is perpendicular to them only in a time-averaged sense. The results of quantum-chemical calculations on isolated molecular dimers and trimers support this conclusion. In addition, the calculation of separate coulombic, dispersion, polarization and repulsion contributions to intermolecular bonding reveals that the C–H$\cdots\pi$-bond interaction between acetylene and benzene in a T-shaped dimer consists of a mixture of coulombic and polarization interactions. In the benzene–acetylene cocrystal, its magnitude is quantitatively comparable with that of other dispersive interactions. 5.4 ns Molecular-dynamics simulations of the liquid mixture reveal that the two components are persistently miscible, a possible key to the formation of the cocrystal. No structure is, however, observed in the solution during the relatively short simulation time.

Introduction. – Chemistry in the past century has been a matter of interatomic-bonding interactions in the range of 200–500 kJ mol^{-1}, the chemistry of the synthesis of new intramolecular bonding patterns, and of new compounds. It may well be said that the third millennium is seeing the emergence of a new chemistry, one concerned with the collective action of many weaker potentials in the range of 5–20 kJ mol^{-1} that cooperate in the stabilization of liquids, crystals, and mesophases. In fact, the classification of intermolecular forces and the possible use of types and categories of intermolecular recognition patterns for assembling and exploiting new molecular aggregates are subjects of wide current interest.

While the practicing chemist may well proceed by repeated trial and error, guided by intuition and a few unifying principles or even rules of thumb, a theory of intermolecular bonding requires that intermolecular forces be recognized and their magnitudes calculated. Structure is dictated by forces, and, therefore, a study of structure is a study of the result of the actions of these forces. The undisputed gold standard of structural analysis is single-crystal X-ray analysis, while a number of theoretical methods are available for the simulation of molecular energies and

[1]) Cocrystallization with acetylene first communicated in [1].

molecular evolution. However, the essential features of intermolecular interactions are better studied on systems made of small molecules. Here, one can more reasonably hope to single out separate effects. This is in perfect consonance with the requirements of theoretical chemistry, where, in many cases, keeping the dimensions of the molecule to a minimum is essential. However, this also clashes with the demands of X-ray diffraction, where well-grown single crystals are required. These can be obtained under ambient conditions only for larger molecules. Thus, there is a need to extend the scope of X-ray crystallography into ranges of temperature and pressure that are far from ambient.

Acetylene is well-suited for cocrystallization studies because it dissolves well in various organic solvents, which indicates its versatility in intermolecular interactions [2]. Both 1:1 and 1:2 complexes with acetone as well as a 2:1 cocrystal with DMSO have been produced. These complexes are expected to resemble a 'frozen' status of the liquid phase [1]. New techniques have been developed to obtain cocrystals with acetylene and to analyze the structures.

We report in this paper the single-crystal growth and X-ray analysis of the 1:1 benzene/acetylene molecular complex. The elucidation of the crystal structure is supplemented with a theoretical study of the free complex and of its crystal structure by quantum-mechanical methods, by a new combined quantum-mechanical/classical method, and by empirical methods; and of the dynamic evolution of the acetylene-benzene mixture by standard molecular-dynamics simulations. The results reveal, we believe, as much as is currently possible, details of the nature and magnitude of intermolecular forces acting in this unusual aggregation motif.

Experimental. – A 0.1 mm diameter quartz capillary was glued vertically, with the widened funnel on top and the closed tip upside down, to a high-vacuum line. A small brass cylinder used to fit into the goniometer head was also glued at the upper end of the capillary and temporarily fixed with a clip, so that *ca*. 20 mm of the closed capillary pointed downwards. This part was immersed in liq. N_2 and the components were condensed one after the other into the capillary at a volumetric ratio of *ca.* 1:1. The capillary was flame-sealed carefully between the brass cylinder and the funnel with a H_2/O_2 microburner. When direct touching of the capillary is avoided and flame sealing is performed carefully, explosion due to internal pressure can be prevented, and we estimate that such capillaries can withstand pressures well in excess of 100 bar. This procedure allows the transfer and fixing of the capillary and of the brass cylinder with the attached clip as a handle to the goniometer head on the diffractometer.

Our *SMART 1000* three-circle diffractometer (*Siemens-Bruker AXS*) was equipped with an *X-Stream LT* device (*Molecular Structure Corporation*), which provides a very stable, vertical cold gas stream (max. $\pm 0.2^\circ$). We inserted an arc with an additional small *x*,*y*,*z*-drive onto the goniometer head, which is usually mounted at a constant χ angle because of the geometry of the goniometer. This allows us to mount the capillary vertically while ϕ is kept constant and scanning is performed only by the ω circle. The data coverage can be reduced, depending on the orientation and the symmetry of the crystal at a detector position in θ at 28.24° (detector distance 4 mm). The advantage, however, is the vertical alignment of the capillary with the cold gas stream, parallel even during data collection. This provided an almost constant temperature of 217 K along the capillary, but also allowed us to produce a locally heated and molten zone at the focus of the CO_2 laser [3]. By computer-controlled movements of the local heating, and observation with a video camera, single crystals could be produced at the interfaces between the gaseous, liquid, and solid phases. Diffraction patterns were recorded from time to time; some of them resulted from superimposed diffraction by different crystals. When possible, these were separated manually by application of the RLATT program in the *Bruker AXS* diffractometer software. This software performs a rotation of all reflections detected in the reciprocal space, and allows selection and separation of data sets belonging to different crystals, finally proceeding to indexing. In the present case, the data contained the patterns of benzene and acetylene, in addition to patterns of unknown crystal dimensions, which later were attributed to the cocrystal of the two. After repeated attempts, we were then able

to grow a cocrystal that almost filled the complete diameter of the capillary (*ca.* 2 mm in length), thus exceeding the diameter of the primary X-ray beam. Data from this crystal were first collected at 201 K and later at 123 K. The rest of the structure determination was according to standard procedures, *i.e.*, LP and empirical absorption corrections, space-group determination, structure solution with direct methods, and structure refinement. Details are given in *Table 1*, bond distances are collected in *Table 2*.

Results. – *X-Ray Diffraction.* The benzene ring lies in a special position of space group $R\bar{3}m$, with D_{3d} point-group symmetry, while the acetylene molecule lies on an axis perpendicular to the center of the benzene plane, also in a special position, as shown in *Fig. 1*. The three dimer pairs in the unit cell are described by the equivalent positions x, y, z, $2/3+x, 1/3+y, 1/3+z$, and $1/3+x, 2/3+y, 2/3+z$.

The benzene C–C distances are in the usual range. There are no obvious peculiarities about the ADPs that might indicate static or dynamic disorder as found for the dibromine–benzene complex [4][5], either at 201 or at 123 K (see *Table 2*). In the latter case, the structure has an axial orientation at 223 K [6] and undergoes a solid-state phase transition upon cooling to 203 K; the deviation from the main axis of benzene is 5.1° at 123 K [4][5]. Our results, however, reveal an unusually short triple bond, which, moreover, undergoes abnormal expansion at lower temperature (1.097(10) Å at 201 K and 1.152(4) Å at 123 K). Lengthening of intramolecular

Table 1. *Crystal Data and Structure-Refinement Details for the 1 : 1 Acetylene/Benzene Complex*

	Temperature/K	
	201	123
Empirical formula	$C_2H_2 \cdot C_6H_6$	
Formula weight/Da	104.14	
Density (calculated)/g cm^{-3}	0.987	1.010
$F(000)$	168	
Crystal size	*ca.* 0.1 mm diameter	
Crystal color	colorless	
Crystal description	cylindric	
Wavelength	0.71073 Å	
Crystal system	trigonal	
Space group	$R3m$	
Unit-cell dimensions		
a/Å	8.586(5)	8.5038(13)
b/Å	8.586(5)	8.5038(13)
c/Å	8.235(4)	8.2061(19)
V/Å^3	525.8(5)	513.92(16)
θ Range for data collection/°	3.69–28.21	
Completeness to $\theta = 28.21°$/%	95.4	97.1
Reflections collected	685	663
Max./min. transmission	not applied	1.00/0.93
R(merg) before/after correction	not applied	0.0514/0.0159
Independent reflections	167 [R(int) = 0.0515]	167 [R(int) = 0.0180]
Data/restraints/parameters	81/0/14	155/0/14
Final R indices [$I > 2s(I)$]	$R1 = 0.0661$, $wR2 = 0.1892$	$R1 = 0.0407$, $wR2 = 0.1093$
R indices (all data)	$R1 = 0.0964$, $wR2 = 0.2393$	$R1 = 0.0436$, $wR2 = 0.1140$
Extinction coefficient	0.06(4)	0.06(2)
Largest diff. peak and hole/e · Å^{-3}	0.267 and −0.159	0.180 and −0.137

Table 2. *Refined Parameters for the 1 : 1 Acetylene/Benzene Crystal Structure*

	Temperature/K	
	201	123
Atom positions		
C(1)	$x=0$, $y=0$, $z=0.4334(6)$	$x=0$, $y=0$, $z=0.4298(3)$
C(2)	$x=0$, $y=0.8400(3)$, $z=0$	$x=0$, $y=0.8366(1)$, $z=0$
H(1)	$x=0$, $y=0$, $z=0.311(12)$	$x=0$, $y=0$, $z=0.312(4)$
H(2)	$x=0$, $y=0.731(3)$, $z=0$	$x=0$, $y=0.7237(18)$, $z=0$
ADPs and U(iso) /Å$^2\cdot 10^3$		
C(1)	U_{11},$U_{22}=97(3)$, $U_{33}=70(3)$, $U_{12}=49(1)$	U_{11},$U_{22}=43(1)$, $U_{33}=35(1)$, $U_{12}=22(1)$
C(2)	$U_{11}=98(2)$, $U_{22}=81(2)$, $U_{33}=61(2)$, $U_{23}=1(1)$, $U_{13}=1(1)$, $U_{12}=49(1)$	$U_{11}=44(1)$, $U_{22}=36(1)$, $U_{33}=28(1)$, $U_{23}=0(1)$, $U_{13}=1(1)$, $U_{12}=22(1)$
H(1)	0.19(3)	0.078(10)
H(2)	0.089(8)	0.048(4)
Distances/Å[a])		
C(1)–C(1)′	1.097(10)	1.152(4)
C(1)–H(1)	1.01(9)	0.97(4)
C(2)–C(2)″	1.373(3)	1.3898(11)
C(2)–H(2)	0.94(3)	0.960(15)

[a]) Symmetry transformations used to generate equivalent atoms: (′) $=-x$, $-y$, $-z+1$; (″) $=x-y+1$, $x+1$, $-z$.

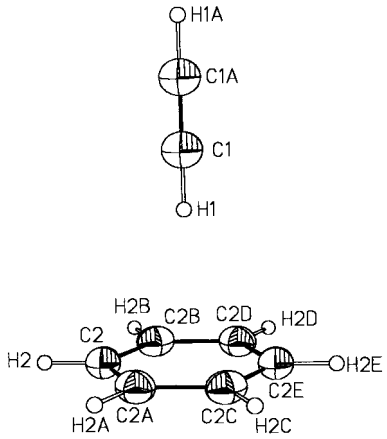

Fig. 1. *The molecular unit in the crystal, with atom numbering*

distances when lowering the temperature is quite a common artifact that can be attributed to thermal motion and to the refinement procedure [7]. Corrections can be performed with the 'rigid-body' approach [8][9] if the anisotropic atoms are not linearly arranged and not positioned on a cone section. Unfortunately, both conditions apply here. Another artifact due to the refinement procedure may appear for atoms at small distances with relatively high electron density between them, resulting in unduly short intramolecular distances. This artifact can be reduced with high-angle refinements or with higher weights for high-angle data [10]. However, comparison of bond

distances among results derived from different methods and refinement procedures would then be improper [11]. Thus, the triple-bond length in the complex is expected to be in the range of 1.17–1.20 Å, as compared to neat acetylene (X-ray at 141 K, 1.176 Å [12]). The triple-bond length in 3-ethynylcyclopropene is 1.184 Å at 103 K [11], longer than the mean distance of 1.174 Å for 367 structures with terminal acetylene groups [13][14], probably because, in the *Cambridge* database, most of the structures were determined at room temperature. In di-(*tert*-butyl)acetylene, the triple-bond length is 1.200 Å at 281 K [15], which compares well with the mean value of 1.194 Å for 1042 structures with a C–C≡C–C fragment [13][14].

In the present complex, all the above considerations suggest an essentially dynamic disorder process, in which the acetylene molecule moves along a double cone between benzene molecules. Assuming 1.20 Å as the 'real' triple-bond length, the deviation from the axial position is 24° for the 201 K structure and 15° for the 123 K structure. Almost the same values (23° and 15°) result from the assumption that the U_{11} to U_{33} ratio is a linear function of temperature, yielding a quite reasonable extrapolated triple-bond distance of 1.192 Å.

The crystal packing is shown in *Fig. 2*. The distance between parallel benzene molecules corresponds to the length of the cell *c*-axis (see *Table 1*), so that, based on the X-ray intramolecular-bond distances for the acetylene molecule, the C–H···π-bond (centroid) distance is 2.447 Å at 123 K and 2.462 Å at 201 K (normalized C–H distances applied). The closest intermolecular C···C distances for the benzene molecules are 5.724 Å (123 K) and 5.839 Å (201 K) and the C(sp^2)···C(sp) contacts are 3.853 Å (123 K) and 3.918 Å (201 K); for more detail, see the later section on packing calculations.

Quantum-Chemical Calculations. Ab initio molecular-orbital calculations on weakly bound systems such as benzene–acetylene complexes place fairly high demands on the

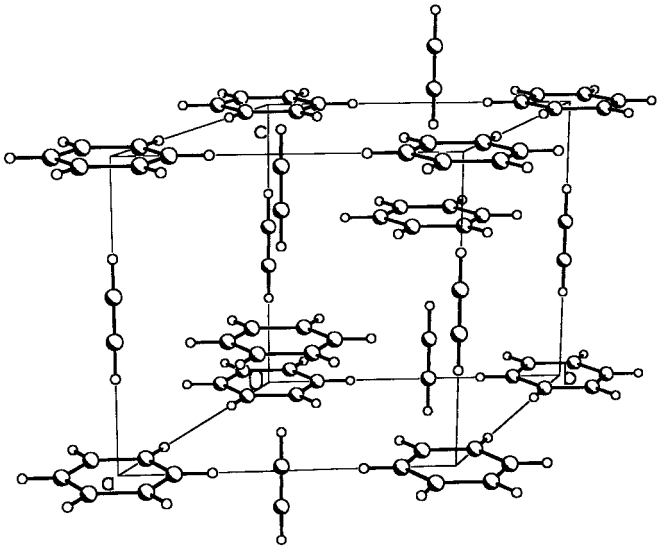

Fig. 2. *A packing diagram of the 1:1 benzene/acetylene cocrystal*

calculational level. Density-functional techniques, while very accurate for many systems, cannot reproduce *Van der Waals* interactions correctly [16] and are, therefore, not applicable to this problem. Similarly, *Hartree-Fock* calculations cannot be expected to reproduce dispersion interactions adequately [17], so we have used second-order *Møller–Plesset* (MP2) perturbation theory [18] to treat electron correlation. MP2 Theory performs relatively well for weak interactions [19]. Geometries were optimized at the MP2 level by means of the 6-31G(d) basis set [20], and single-point calculations to refine the calculated interaction energies were performed at the MP4sdtq [21] with the diffuse-augmented 6-31 + G(d) basis set [22] to minimize basis-set superposition error. The 1:1 acetylene/benzene complex was investigated in C_{6v} symmetry and the 1:2 acetylene/benzene complex in D_{6d} and D_{6h}. All calculations were performed with Gaussian98 [23].

The geometries, energies and frequencies calculated for the two types of acetylene:benzene complex are shown in *Table 3*. The geometries of the benzene and acetylene moieties are hardly affected by complex formation. The changes in bond lengths are on the order of 10^{-3} Å. The distance from the acetylene H-atom to the center of the benzene ring is 2.367 Å for the 1:1 and 2.383 for the 2:1 acetylene/benzene complex. The calculated interaction energy between the acetylene and one benzene unit is 12.6 kJ mol^{-1} (MP4sdtq/6-31 + G(d)//(MP2/6-31G(d) + MP2/6-31G(d)

Table 3. *MP2/6-31GF(d) Optimized Geometries, Energies, and Frequencies of the Normal Vibrations for the Acetylene/Benzene Complexes.* MP4sdtq/6-31 + G(d) total and complexation energies are also shown.

	Acetylene/benzene		
	1:1	1:2	1:2
Symmetry	C_{6v}	D_{6d}	D_{6h}
C≡C/Å	1.218	1.219	1.219
C–C (C_6H_6)/Å	1.398	1.397	1.397
≡C–H/Å	1.067[a]), 1.066	1.067	1.067
C–H (C_6H_6)/Å	1.087	1.087	1.087
(C_6H_6)···H–C≡/Å	2.367	2.383	2.383
θ (C_6H_6)/° [b])	0.07	0.03	0.03
E(tot)/a.u.	− 308.53032	− 539.99343	− 539.99343
ΔE/kJ mol^{-1}[c])	− 11.3	− 21.8	− 21.8
ZPE/kJ mol^{-1}[d])	335	603	603
Frequency/cm^{-1}			
ν_1	E_1, 42.2	A_1, 1.5 (imaginary)	A_{1u}, 1.5 (imaginary)
ν_2	E_1, 83.6	E_2, 11.9	E_{1u}, 11.9
ν_3	A_1,90.2	E_2, 44.2	A_{1g}, 44.2
ν_4		E_1, 44.4	E_{1g}, 44.4
ν_5		E_1, 73.4	E_{1u}, 73.4
ν_6		E_2, 95.8	E_{1g}, 96.0
ν_7		A_2,115.9	A_{2u}, 115.9
MP4sdtq/6-31 + G*//(MP2/6-31G*)			
E(tot)/a.u.	− 308.71687	− 540.31855	− 540.31853
ΔE/kJ mol^{-1}[c])	− 12.6	− 25.5	− 25.5

[a]) H-atom closest to acetylene. [b]) Out-of-plane angle for benzene H-atoms. [c]) Complexation energy at the relevant level corrected for the zero-point vibrational energy. [d]) Zero-point vibrational energy calculated on the basis of the harmonic approximation.

zero point vibrational energy), for both the dimer and trimer models. The calculated low-energy normal modes are shown in *Fig. 3*. The trimolecular complex has an imaginary frequency corresponding to an in-plane rotation of the benzene rings; the next three vibrations in order of ascending frequency are a 'jaw-opening', an 'acetylene-benzene bond stretch', and an 'acetylene wobbling' mode. Any combination of these three low-frequency modes characterizes the complex as an extremely floppy one; the acetylene molecular vector and the vectors perpendicular to the two benzene planes are parallel only in a time-averaged sense.

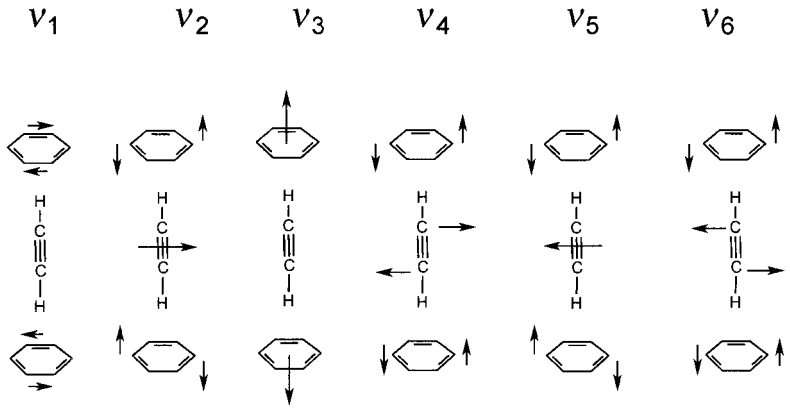

Fig. 3. *The low-frequency normal modes of the T-shaped trimer complex.* The corresponding frequencies are given in *Table 3*.

A further calculation of intermolecular energies was performed with the SCDS (semi-classical density sums) method [24][25]. Briefly, the method consists of obtaining first the electron density for each separate molecule in a supramolecular entity by standard quantum-chemical methods; then, the coulombic, polarization, and dispersion energies are calculated as sums over contributions from each pair of electron-density pixels in separate molecules. The repulsion energy is evaluated through the overlap between the densities. The total intermolecular energy is then taken as the sum of the coulombic, polarization, dispersion, and repulsion terms. The method has been calibrated to reproduce the cohesive energies of some molecular dimers and the heats of sublimation of a variety of organic crystals [25]. To obtain the electron density, an MP2/6-31G** molecular-orbital calculation was carried out [23] for the benzene and acetylene molecules (geometries: benzene, C–C 1.3738 Å, C–H 1.0793 Å, all angles 120°; linear acetylene, C–C 1.20, C–H 1.06 Å). ESP Atomic charges were C(benzene): −0.112, H(benzene): +0.112, C(acetylene): −0.24, H(acetylene): +0.24 electrons. The valence charge density was calculated on a grid of $120 \times 120 \times 100$ points (benzene) and $100 \times 100 \times 120$ points (acetylene).

The SCDS method was first applied to the calculation of the intermolecular energies in the isolated 1:2 acetylene/benzene complex, with a fixed benzene–benzene distance of 8.235 Å as results from the X-ray study, varying the tilt angle of the acetylene molecule. This analysis (*Fig. 4,a*) shows that dispersion energy is by far the largest contribution to the stabilization of the complex, followed by *Coulomb* and

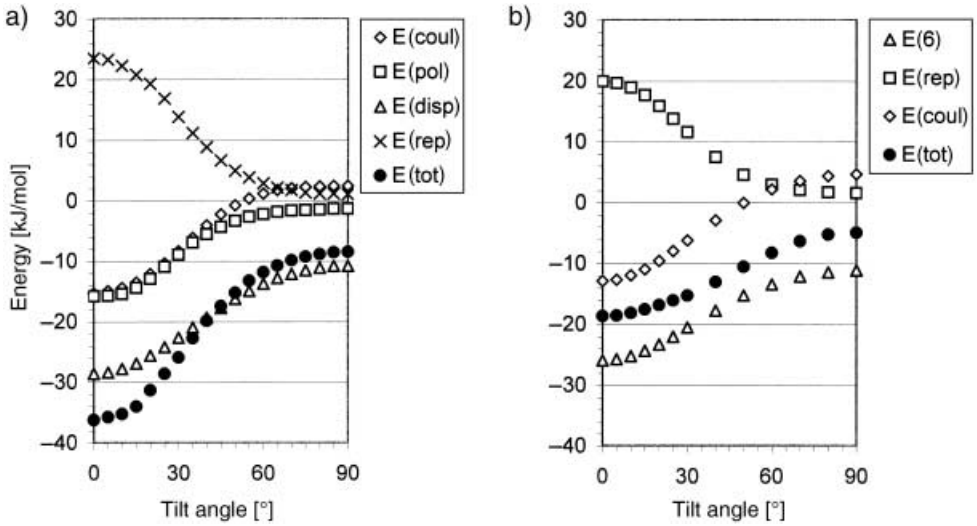

Fig. 4. a) *The SCDS results for the coulombic, polarization, dispersion and repulsion energies in the T-shaped trimer shown in* Fig. 3, *as a function of the acetylene tilt angle* (angle between the acetylene line and the line connecting the two benzene ring midpoints). The acetylene center of mass is fixed at the midpoint of the vector joining the benzene ring centers. b) *The force-field energy components for the same tilt, repulsion, coulombic, and* r^{-6}.

polarization energies. The acetylene tilt is essentially unrestricted up to about 15°. The overall result is, thus, consistent with the picture given by the normal-mode calculations; an essentially free wobbling motion of the acetylene molecule out of the vertical line joining the two benzene rings even at low temperatures (remember that kT/hν is about 1.5 for a 50 cm^{-1} vibration at 100 K). The SCDS calculated cohesive energy of 36 kJ mol^{-1} is somewhat larger than the one obtained by the correlated MO calculation in *Table 3*.

To shed further light on the possible origin of the peculiar complex observed here, the SCDS interaction energy was calculated also for a 'hot-dog' complex, in which the acetylene molecule in positioned horizontally halfway between two benzene rings. The minimum energy distance between the benzene rings is, in this case, 6.8 Å. The total complexation energy is only -14.9 kJ mol^{-1}, much smaller than for the vertical acetylene complex; the coulombic energy is destabilizing ($+2.7$ kJ mol^{-1}), and the complex is stabilized by a large dispersion contribution (-32.6 kJ mol^{-1}) and by a smaller polarization component (-3.5 kJ mol^{-1}) against a repulsion energy of $+18.5$ kJ mol^{-1}.

In the cocrystal, the nearest neighbors are arranged as shown in *Fig. 5*. Unfortunately, the density-sums computer program does not allow treatment of the full symmetry of a crystal with two molecules in the asymmetric unit, so that the complete lattice energy cannot be calculated. However, a calculation was run for the 13-dimer crystal cluster shown in *Fig. 6*, and the total energy was then partitioned over molecule-molecule contributions. This partitioning allows us to judge the relative importance of the various energy contributions to the stabilization of the crystal. The

main stabilizing factor (refer to *Figs. 5* and *6*, and to *Table 4*) comes from benzene-acetylene coulombic and dispersion interactions (**A**–**A**′). Next comes a predominantly dispersive offset-stacked benzene-benzene interaction (**A**–**B**), followed by the lateral interaction between an acetylene and a benzene molecule (**A**′–**B**). Parallel acetylene-acetylene and second-neighbor benzene-benzene interactions play only a minor role. All coulombic interactions between parallel molecules related by lattice translations (**D**–**F** in *Fig. 6*) are slightly destabilizing.

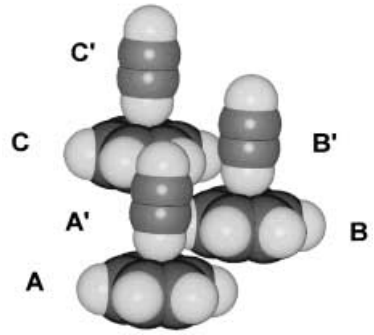

Fig. 5. *The basic packing motif of first neighbors in the 1:1 benzene/acetylene cocrystal.* Labels (unprimed for benzene, primed for acetylene molecules) refer to energies in *Table 4*. Graphics by SCHAKAL [26].

Table 4. *Energy Partitioning for the Intermolecular Interactions in* Figs. 5 *and* 6.

Interaction	Distance between centers of mass /Å	E(coul)/ kJ mol^{-1}	E(disp)/ kJ mol^{-1}	E(rep)/ kJ mol^{-1}
A–**A**′	4.118	– 7.9	– 12.7	11.7
A–**B**	5.666	– 3.0	– 9.0	5.8
A′–**B**	5.144	– 2.3	– 5.9	6.9
A′–**B**′	5.666	– 0.3	– 0.4	0.0
A–**C**	7.397	– 0.1	– 0.6	0.0
A′–**C**′	7.397	– 0.2	– 0.1	0.0
D–**E**	8.235	+ 0.3	– 0.2	0.0
E–**F**	8.586	+ 0.2	– 0.5	0.0
D′–**E**′	8.235	+ 0.5	– 0.1	0.0

Polarization energies cannot be apportioned over molecule-molecule contributions because they are many-body energies, as they depend on the electric field of all surrounding molecules. The order of magnitude of the polarization energy generated at the central benzene molecule in the cluster of *Fig. 6* is – 11.9 kJ mol^{-1}, and that at the central acetylene molecule is – 8.4 kJ mol^{-1}.

Force-Field (FF) *Calculations.* In a much simpler and more approximate approach, intermolecular energies can also be calculated by empirical force fields:

$$E(i,j) = A\ \exp(-Br_{ij}) - C(r_{ij})^{-6} + q_i q_j / r_{ij} \quad (1)$$

or

$$E(i,j) = A\ (r_{ij})^{-12} - C(r_{ij})^{-6} + q_i q_j / r_{ij} \quad (2)$$

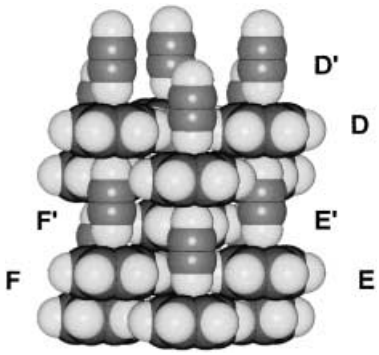

Fig. 6. *The 13-dimers molecular cluster used to simulate the whole crystal structure in SCDS calculations.* Labels (unprimed for benzene, primed for acetylene molecules) refer to energies in *Table 4*. Graphics by SCHAKAL [26].

where $E(i,j)$ is the energy contribution between two atoms in different molecules, r_{ij} is their separation, A, B, and C are empirical parameters for each atom type, and the q's are parametric 'charges' formally located at atomic nuclei. The lattice energy for the acetylene (orthorhombic low-T phase [27]) and benzene (at 218 K [28]) crystals and for the acetylene-benzene cocrystal whose structure has been determined in this work were evaluated by means of the *Williams* [29], and UNI-q parameter sets [30][31]. In both cases, the last term in the above equation was calculated by ESP 'charges' (or charges which, disseminated at the location of atomic nuclei, are supposed to mimic as best as possible the molecular electrostatic field). The three crystal structures were also energy-optimized under the action of these two force fields; results are shown in *Table 5*.

The conclusion to be drawn from these results is that the UNI-q parameters perform slightly better than those of *Williams* in that structure deformations after optimization are much smaller. Calculated lattice energies are close to the exper-

Table 5. *Calculated Lattice Energies Before and After Optimization, Rigid-Body Angular-Shift, Cell-Dimension Variations, and Overall Discrepancy Factor*

	E(before)/ kJ mol^{-1}	E(after)/ kJ mol^{-1}	$\Delta\theta$/°	Δa/%	Δb/%	Δc/%	r [29]
Acetylene							
UNI-q	– 21.3	– 22.2	9	2	– 1	– 4	43
Williams	– 14.0	– 18.4	7	9	5	0	109
ΔH(subl)	23.5						
Benzene							
UNI-q	– 48.5	– 49.6	2	– 2	– 1	– 2	11
Williams	– 42.9	– 44.6	3	1	1	4	17
ΔH(subl)	44.4						
Cocrystal							
UNI-q	– 73.0	– 78.0	–	– 6	-	2	65
Williams	– 56.4	– 66.0	–	– 2	–	8	84

imental heats of sublimation [32]. The *Williams* parameters perform better for benzene and the UNI-q parameters better for acetylene.

The intermolecular energy was evaluated by the force-field (FF) method also for the isolated 1:2 acetylene/benzene complex (see *Fig. 4, b*). The FF repulsion energy is strikingly similar to the SCDS one, while the SCDS coulombic energy is slightly larger than the point-charge r_{ij}^{-1} term because of penetration effects. The r_{ij}^{-6} FF term is about one-half the sum of dispersion and polarization terms, so that the total FF cohesive energy is only -19 kJ mol^{-1}, rather smaller than the value obtained from the correlated MO calculation and about one-half that obtained by the SCDS method.

Molecular-Dynamics Calculations. Molecular-dynamics (MD) calculations were performed in an attempt to evaluate the miscibility of acetylene and benzene, the two components of the liquid mixture from which the cocrystals were grown. The intermolecular force field used was UNI-q, after the results presented above; the GROMOS96 program package [33] was used. A computational box with 256 acetylene and 256 benzene molecules in random orientations was prepared as a starting system, and a few thousand energy-minimization cycles were performed to dispose of unrealistically close contacts. MD Calculations were performed in the NPT ensemble (constant number of particles, temperature, and pressure; cutoff for intermolecular interactions 10 Å; for other details, see previous work as described in the discussion section). The system was first warmed to 100 K and then to 200 K. After some starting runs and a 200 ps preliminary equilibration run, the liquid mixture was simulated at constant $T = 200$ K for 800 ps at 1 bar, and then for 200 ps at 10 bar, for 200 ps at 50 bar, for 1 ns at 200 bar and finally for 3 ns at 500 bar. The total simulation time is, thus, 5.4 ns.

Three separate radial-distribution functions were evaluated for the benzene-benzene (**BB**), benzene-acetylene (**BA**), and acetylene-acetylene (**AA**) centers of mass:

$$g(r_k) = n(r_k)/\ (4\pi r_k^2 \mathrm{d}r) \tag{3}$$

where k = **AA**, **AB**, or **BB**, $n(r)$ is the number of distances in a spherical shell centered at r and with thickness dr (here taken as 0.3 Å). To describe the possible molecular alignment leading to the observed cocrystal, molecular-orientation vectors were defined, *viz*. the vector along the acetylene molecule and the vector perpendicular to the benzene ring. The three angular-distribution functions were:

$$g(\theta)_k = [n(\theta)_k/\sin(\theta)_k] \tag{4}$$

$$g'(\theta)_k = g(\theta)_k/\langle g(\theta)_k \rangle \tag{5}$$

$n(\theta)$ is the number of angles in a range centered at θ and with a width of 3°, and the radial function is empirically weighted by the reciprocal of $\sin(\theta)$ to account for the increase in the number of possible approaches with increasing θ. The final displayed radial function $g'(\theta)$ is normalized by dividing by the average value of $g(\theta)$. Demixing would be announced by a decrease of $g(r)_{AB}$ and an increase of $g(r)_{AA}$ and $g(r)_{BB}$. Formation of the observed complex would be announced by an increase in the number

of parallel molecular vectors; the relevant alignment function was defined as the sum of the first five slots in each of the three $g'(\theta)$ functions, or an increase of the number of vectors parallel within 15°.

Table 6 shows the numerical results of the simulations. At 200 K and 1 bar, the total cohesive energy (an estimate of the vaporization enthalpy) is 49.7 kJ mol^{-1}, and the density is 0.833 g cc^{-1}. While there is no way to check these calculated numbers against experiment, we believe they are reliable because of the reliability of the force field. These results are at least consistent with the rules of thumb that the enthalpy of vaporization is *ca.* two-thirds of the enthalpy of sublimation (see *Table 5*), and that the decrease in density from crystal to liquid is 10–15% (the crystal density is 0.987 g cm^{-3} at 217 K).

Table 6. *Numerical Results of the MD Simulations*

P /bar	E(tot) / kJ mol^{-1}[a])	E(intra)/ kJ mol^{-1}	E(coul)/ kJ mol^{-1}	E(6–12)/ kJ mol^{-1}	Density /g cm^{-3}
1	– 1478	– 18	– 8.2	– 41.5	0.833
10	– 1454	– 18	– 8.2	– 41.4	0.833
50	– 1507	– 18	– 8.2	– 41.8	0.836
200	– 1687	– 17	– 8.4	– 42.1	0.846
500	– 1960	– 17	– 8.6	– 42.9	0.862

[a]) Total energy of the 256-molecule computational box.

Fig. 7 shows the energy trajectories during the MD simulation. All simulations are seen to be well-equilibrated, and steps are observed only at times of large pressure increases. Correspondingly, *Fig. 8* shows the calculated density profile, with the expected increase as pressure is increased. Molecular dynamics is, in this respect, a source of reliable data that would be impossible or at least extremely difficult to obtain experimentally.

Fig. 9 shows the radial-distribution functions at the ends of the simulations. The shape of these functions is constant throughout, and the mixture seems to be pretty well homogeneous even after (at least, computationally) long simulations. For perfectly random orientation, the alignment function would be the sum of five unit terms, and, therefore, any preferential alignment would be represented by a significant increase of the function from this value. This is not observed in *Fig. 10*, and we must, therefore, conclude that there is still no sign of alignment leading to crystallization, or even to preliminary nucleation, in our simulation after more than 5 ns.

Discussion and Conclusions. – A crystalline mixture of benzene and acetylene was made and a single crystal of the bimolecular complex was grown *in situ* on the diffractometer where X-ray data could be collected successfully. These results further confirm the versatility of the crystal growing and diffraction facilities at Essen, and the results of the structural analysis reveal the importance and the stimulating influence of research into the intermolecular interactions of binary mixtures, even rather exotic ones.

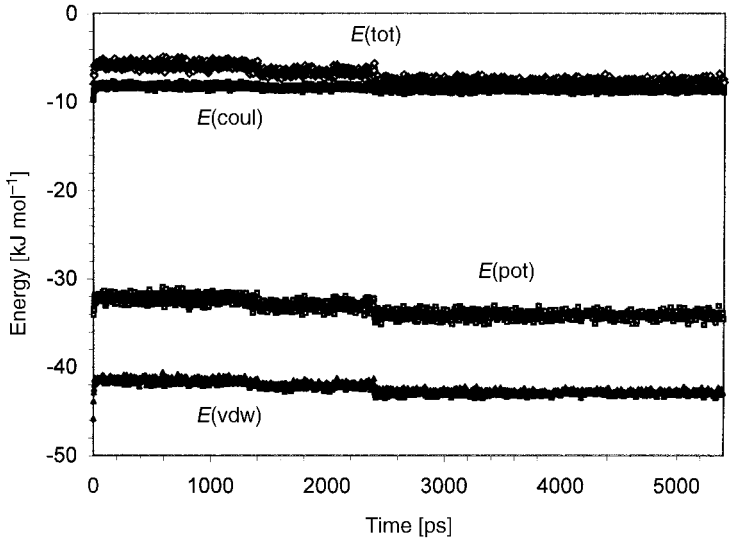

Fig. 7. *Energy trajectories from the MD simulation.* See text for the corresponding temperatures and pressures. Energies per molecule: total, total potential (pot), coulombic (coul), and 6–12 (vdW).

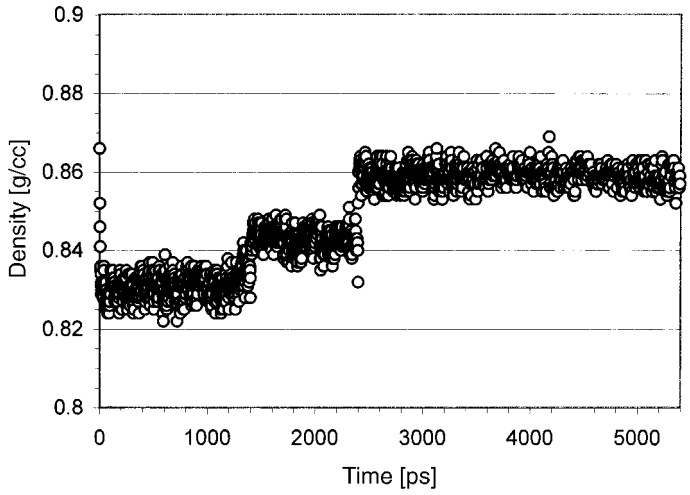

Fig. 8. *The density profile during the MD simulation in* Fig. 7

In the dimer and trimer benzene–acetylene complexes, the intramolecular geometries resulting from quantum-chemical calculations agree well with those observed by single-crystal X-ray diffraction. Calculations performed by three different approaches, a molecular-orbital calculation including electron correlation, a semi-classical method based on the calculated electron density, and even purely empirical force-field methods, agree with the results of X-ray-diffraction experiment. They all indicate a wobbling motion of the acetylene in the crystal between the two benzene

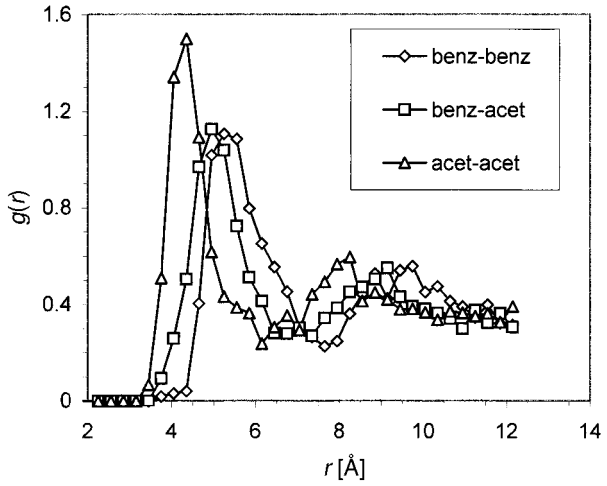

Fig. 9. *The benzene-benzene, benzene-acetylene, and acetylene-acetylene radial-density functions at the end of the MD simulation in* Fig. 7

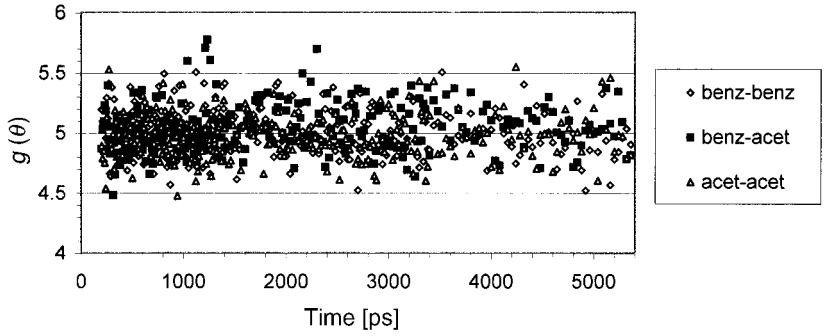

Fig. 10. *The benzene-benzene, benzene-acetylene, and acetylene-acetylene alignment functions* (see text for definition) *during the MD simulation in* Fig. 7. Completely random orientation corresponds to a value of 5.

rings to which it is perpendicular. The total calculated cohesive energy is 26 kJ mol^{-1} by the molecular-orbital method, 19 kJ mol^{-1} by the force-field method, and 36 kJ mol^{-1} in the semiclassical approach. The latter is known [25] to overestimate the lattice energy of pure benzene by about 7%, so it is likely that the cohesive energy is also overestimated.

The benzene-acetylene mode of recognition in the cocrystal described here could be called the paradigm of the weak C–H$\cdots\pi$-bond interaction [34]. An analysis of the various energy types in the free trimer complexes, the T-shaped one observed in the crystal and the 'hot-dog' one, where the acetylene molecule is parallel to the benzene rings, reveals that the largest cohesive contribution is, in both cases, a dispersion energy of about 33 kJ mol^{-1}. However, in the T-shaped trimer, the coulombic component is substantially stabilizing, whereas it is destabilizing in the hot-dog trimer. Together with the larger coulombic component, there is also a larger polarization component of 15 kJ

mol^{-1} in the T-shaped trimer, against 3.5 kJ mol^{-1} in the hot-dog trimer. On the basis of these comparisons, we conclude that what drives benzene and acetylene to the observed T-shaped arrangement, the $C-H\cdots\pi$-bond interaction, is to a first approximation a coulombic and polarization interaction between the electron-deficient H-atom end of the acetylene molecule and the electron-rich core of the benzene ring. Polarization energies are nearly always neglected in empirical or semi-empirical force fields, in the assumption that they are small and covariant with coulombic energies. We can confirm the second part of this hypothesis in this case but not the first. Polarization energies are of the same order of magnitude as coulombic energies in this example.

When the whole crystal structure is considered, however, things become more complicated. The quantitative calculation of molecule-molecule energies shows that the benzene-benzene stacking energy, a mainly dispersive interaction, is almost on the same level of importance as the benzene-acetylene interaction. Moreover, polarization energies are also of the same order of magnitude as the differences in energy between several molecule-molecule arrangements. It is very likely that the T-shaped interaction mode with its large coulombic, long range component is preferred at the preliminary stages of aggregation. Nevertheless, the spacial compatibility of neighboring T-shaped trimers, when the benzene ring of one fits into the hollow space between the two rings of the other, produces a favorable lateral benzene-acetylene arrangement that may also be relevant in determining the final overall packing.

Molecular-dynamics simulations show that no demixing of the acetylene and benzene liquid phases occurs within a 5 ns period. This may be compared with the case of the acetic acid [35] and succinic anhydride [36] solutions in CCl_4, where aggregation of the solute into plurimolecular micelles was promptly observed, even in shorter simulations. Clearly, neither the enthalpic nor the excluded-volume factors are strong enough to force separation of acetylene and benzene over a short time period as observed for mixtures of polar solutes and a nonpolar solvent like CCl_4. Pressure does not seem to be a factor here. Judging from these results, the driving force for formation of the cocrystal can be traced back to the persistent miscibility of the two components.

At the same time, no preferential alignment of either separate component molecules or heteromolecular complexes is observed over the same period of time. One would, indeed, be surprised if it were, as it is almost certain that structuring of molecular assemblies into recognizable geometric patterns requires much longer times and a careful choice of temperature, saturation and, possibly, pressure conditions.

REFERENCES

[1] R. Boese, M. T. Kirchner, W. E. Billups, L. R. Norman, *Angew. Chem., Int. Ed.* **2003**, in press.
[2] P. Hölemann, R. Hasselmann, *Chem. Ing. Tech.* **1953**, *25*, 466.
[3] R. Boese, M. Nussbaumer, in 'Organic Crystal Chemistry' Ed. J. B. Garbarczyk, D. W. Jones, Oxford University Press, Oxford, 1994, p. 20–37; www.ohcd-system.com.
[4] A. V. Vasilyev, S. V. Lindemann, J. K. Kochi, *Chem. Commun.* **2001**, 909.
[5] A. V. Vasilyev, S. V. Lindemann, J. K. Kochi, *New. J. Chem.* **2002**, *26*, 582.
[6] O. Hassel, K. O. Stromme, *Acta Chem. Scand.* **1958**, *12*, 1146.
[7] R. Boese, in 'Advances in Strain in Organic Chemistry', Vol. II, Ed. B. Halton, JAI Press, Greenwich, 1992, p. 191–254.
[8] J. D. Dunitz, E. F. Maverick, K. N. Trueblood, *Angew. Chem., Int. Ed.* **1988**, *27*, 880.
[9] J. D. Dunitz, *Chem. Commun.* **1999,** 2547.

[10] P. Seiler, J. D. Dunitz, *Acta Crystallogr. B* **1979**, *35*, 2020.
[11] K. K. Baldridge, B. Biggs, D. Bläser, R. Boese, M. M. Haley, A. H. Maulitz, J. S. Siegel, *Chem. Commun.* **1998**, 1137.
[12] G. J. H. van Nes, F. Bolhuls, *Acta Crystallogr.* **1979**, *B35*, 2580.
[13] F. H. Allen, *Acta Crystallogr. B* **2002**, *58*, 380.
[14] I. J. Bruno, J. C. Cole, J. P. M. Lommerse, R. S. Rowland, R. Taylor, M. L. Verdonk, *J. Comput.-Aided Molec. Des.* **1997**, *11*, 525.
[15] R. Boese, D. Bläser, R. Latz, A. Bäumen, *Acta Crystallogr.* **1999**, *C55*, QA0089
[16] C. Adamo, V. Barone, *J. Chem. Phys.* **1998**, *108*, 664.
[17] A. Dalgarno, W. D. Davison, *Adv. Atom. Mol. Phys.* **1966**, *2*, 1.
[18] C. Møller, M. S. Plesset, *Phys. Rev.* **1934**, *46*, 618; J. A. Pople, J. S. Binkley, R. Seeger, *Int. J. Quantum Chem., Symp.* **1976**, *10*, 1.
[19] G. Chalasiski, M. M. Szczeiak, *Chem. Rev.* **1994**, *94*, 1723; B. Jeziorski, R. Moszynski, K. Szalewicz, *Chem. Rev.* **1994**, *94*, 1887; J. F. Dobson, K. McLennan, A. Rubio, J. Wang, T. Gould, H. M. Le, B. P. Dinte, *Aust. J. Chem.* **2001**, *54*, 513.
[20] P. C. Hariharan, J. A. Pople, *Chem. Phys. Lett.* **1972**, *16*, 217.
[21] R. Krishnan, M. J. Frisch, J. A. Pople, *J. Chem. Phys.* **1980**, *72*, 4244.
[22] G. W. Spitznagel, T. Clark, J. Chandrasekhar, P. v. R. Schleyer, *J. Comput. Chem.* **1982**, *3*, 363.
[23] M. J. Frisch, G. W. Trucks, H. B. Schlegel, G. E. Scuseria, M. A. Robb, J. R. Cheeseman, V. G. Zakrzewski, J. A. Montgomery Jr., R. E. Stratmann, J. C. Burant, S. Dapprich, J. M. Millam, A. D. Daniels, K. N. Kudin, M. C. Strain, O. Farkas, J. Tomasi, V. Barone, M. Cossi, R. Cammi, B. Mennucci, C. Pomelli, C. Adamo, S. Clifford, J. Ochterski, G. A. Petersson, P. Y. Ayala, Q. Cui, K. Morokuma, D. K. Malick, A. D. Rabuck, K. Raghavachari, J. B. Foresman, J. Cioslowski, J. V. Ortiz, A. G. Baboul, B. B. Stefanov, G. Liu, A. Liashenko, P. Piskorz, I. Komaromi, R. Gomperts, R. L. Martin, D. J. Fox, T. Keith, M. A. Al-Laham, C. Y. Peng, A. Nanayakkara, C. Gonzalez, M. Challacombe, P. M. W. Gill, B. Johnson, W. Chen, M. W. Wong, J. L. Andres, C. Gonzalez, M. Head-Gordon, E. S. Replogle, J. A. Pople, Gaussian98, Revision A.7, *Gaussian, Inc.*, Pittsburgh, 1998.
[24] A. Gavezzotti, *J. Phys. Chem. B* **2002**, *106*, 4145.
[25] A. Gavezzotti, *J. Phys. Chem. B* **2003**, *107*, 2344.
[26] E. Keller, SCHAKAL92, 'A Program for the Graphic Representation of Molecular and Crystallographic Models', University of Freiburg, 1993.
[27] R. K. McMullan, A. Kvick, P. Popelier, *Acta Crystallogr. B* **1992**, *48*, 726.
[28] G. A. Jeffrey, J. R. Ruble, R. K. McMullan, J. A. Pople, *Proc. R. Soc. London Ser. A.* **1987**, *414*, 47.
[29] D. E. Williams, R. Starr, *Comput. Chem.* **1977**, *1*, 173.
[30] G. Filippini, A. Gavezzotti, *Acta Crystallogr. B* **1993**, *49*, 868.
[31] A. Gavezzotti, G. Filippini, *J. Phys. Chem.* **1994**, *98*, 4831.
[32] J. S. Chickos, in 'Molecular Structure and Energetics, Vol. 2: Physical Measurements', Eds. J. F. Liebman, A. Greenberg, VCH, New York, 1987.
[33] W. R. P. Scott, P. H. Hunenberger, I. G. Tironi, A. E. Mark, S. R. Billeter, J. Fennen, A. E. Torda, T. Huber, P. Kruger, W. F. van Gunsteren, *J. Phys. Chem. A* **1999**, *103*, 3596.
[34] G. R. Desiraju, T. Steiner, 'The Weak Hydrogen Bond in Structural Chemistry and Biology', Oxford University Press, Oxford, 1999.
[35] A. Gavezzotti, *Chem.–Eur. J.* **1999**, *5*, 567.
[36] V. Ferretti, P. Gilli, A. Gavezzotti, *Chem.–Eur. J.* **2002**, *8*, 1710.

Received February 1, 2003